Eco+Rceb

Eco-efficient recycled cement compressed earth blocks

FCT Project

PTDC/ECI-CON/0704/2021

Report Eco+RCEB/R1

Characterisation of materials: soils from Montemor-o-Novo

March 2023

FCT Fundação para a Ciência e a Tecnologia

MINISTÉRIO DA CIÊNCIA E DO ENSINO SUPERIOR Portugal

Eco-efficient recycled cement compressed earth blocks

FCT Project

PTDC/ECI-CON/0704/2021

Report Eco+RCEB/R1

Characterisation of materials: Soils from Montemor-o-Novo

Acknowledgements

The authors wish to thank the Portuguese Foundation for Science and Technology (FCT) for funding this research through project PTDC/ECI-CON/0704/2021, CERIS for supporting this research, Oficinas do Convento – Montemor-o-Novo and SECIL for supporting the experimental work and suppling the materials for the experimental campaign.

Written by

This report has been written by: Sofia Real, Ricardo Cruz, Andrea Balboa, Manuel F.C. Pereira and José Alexandre Bogas.

Information

Main Contractor:

Instituto Superior Técnico, Technical University of Lisbon

Department of Civil Engineering and Architecture

Av. Rovisco Pais, 1049-001 Lisbon, Portugal

Main Research Unit:

CERIS is an FCT-registered research unit, hosted by the Department of Civil Engineering, Architecture and Georesources (DECivil) of Instituto Superior Técnico (IST), University of Lisbon (ULisboa).

Table of Contents

List of Figures

List of Tables

Preface

Although it is estimated that more than 30% of the world's population still inhabit earthen dwellings, in the last two centuries earth has fallen into disuse, due to the emergence of new building materials and construction techniques. However, in line with the increasing demand of more sustainable and eco-friendly building materials, earth construction has regained interest. The low environmental impact and embodied energy, the high availability of raw material, the recyclability, the high hygrothermal comfort, the improved indoor environmental quality, with nearly zero hazardous emissions, and the advances in new construction methods and in the materials science, are some reasons that contributed to the resurgence of earth construction.

A promising approach to earth building materials is the compressed stabilised earth blocks (CSEB), increasing the processing speed and showing improved mechanical strength and durability when stabilised with cementitious materials, such as ordinary Portland cement or hydraulic lime. However, despite its adequate behaviour in real exposure conditions, this type of CSEB fails to address the sustainability issue, since it requires a considerable amount of non-eco-friendly stabilisers.

Alternative more sustainable natural stabilisers have been explored by various investigators, but they are still far from being technically viable and from providing comparable mechanical and durability performance as cementitious materials.

In this context, the low-carbon thermoactivated recycled cement is expected to be a very promising alternative for CSEB stabilisation, potentially providing adequate binding properties with reduced environmental impact. Comparing to conventional cement stabilisers, the new eco-efficient binder contributes to a lower consumption of natural resources and, potentially, over 60% reduction of CO_2 emissions, while adequately repurposing construction and demolition waste.

Therefore, the main objective of this project is the innovative production and characterisation of more eco-friendly CSEB, by using low embodied energy recycled cement from concrete waste as a more sustainable stabiliser. The idea is to also explore the incorporation of construction and demolition waste as partial earth replacement, further increasing the CSEB sustainability.

The new CSEB will be characterised in terms of their main physical, mechanical, thermal and durability properties by means of laboratory tests, as well as in-situ tests involving the long term exposure of various CSEB walls to different natural environments.

In addition, the project also aims the development and characterisation of new more eco-efficient masonry earth mortars for CSEB joints, using recycled cement.

Finally, the best compromise between the technical performance and eco-efficiency of this new CSEB product is assessed by economic and environmental life-cycle analysis.

For the accomplishment of these objectives, a comprehensive experimental program was defined involving the following six main tasks: production of compressed earth blocks stabilised with recycled cement; masonry earth mortar characterisation and CSEB wall production; physical, mechanical and microstructural characterisation of CSEB; thermal performance of CSEB; durability of CSEB; life-cycle cost and life-cycle assessment of CSEB.

1. Introduction

The present study is part of FCT research project, PTDC/ECI-CON/0704/2021, which consists on the production and characterisation of an eco-efficient compressed stabilised earth block, contributing for the resurging interest and confidence in using earth materials, towards a more eco-friendly and sustainable construction practice.

This report presents the characterisation of the soils from Montemor-o-Novo to be used in the production of the compressed stabilised earth blocks (CSEB).

2. Soil characterisation

For this study, 5 soils were selected, with the following designations – *Cortiçadas de Lavre*; *Baldios*; *Amendonça*; *Pinheiro*; *Maja* – which were collected from a homestead nearby Montemor-o-Novo, Portugal. The soils were characterised in terms of their *Atterberg* limits, dry density, particle size distribution, optimum water content and organic matter, as well as through x-ray diffraction and thermogravimetric analysis.

2.1 Particle size distribution

The particle size distribution was determined according to LNEC specification E 239 [1]. A soil sample of approximately 1 kg was placed in a ventilated oven at 105-110ºC, until constant mass. Then, the soil sample clods were broken apart with a mortar and a pestle (Figure 1a) without reduction in the size of the particles as indicated in the LNEC specification E 195 [2]. After this, the samples were sieved in descending order until sieve #10, recording the mass retained in each sieve (Figure 1b). The fraction that passed the sieve #10 was washed in a sieve #200 with a water jet and then dried in a ventilated oven at 105-110ºC, until constant mass. After drying, this soil fraction was passed through sieves #10 to #200 in descending order of size, recording the mass retained in each. Figure 2 presents the obtained granulometric curves.

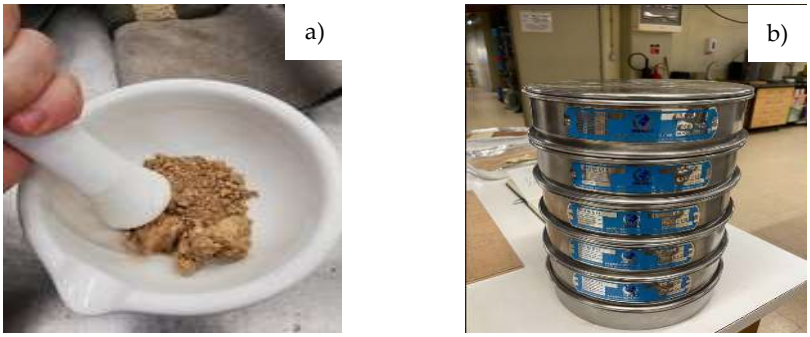

Figure 1 – Particle size distribution: a) breaking of soil sample clods; b) sieve series

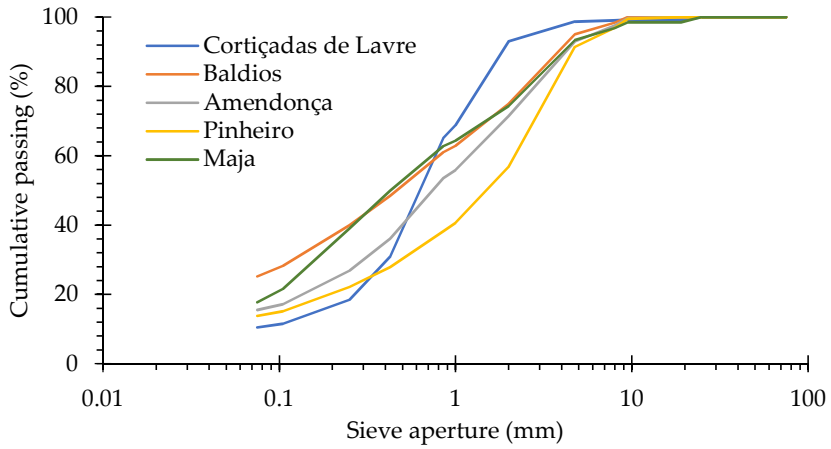

Figure 2 – Granulometric curve of the selected soils

The granulometric curves show that *Cortiçadas de Lavre* had very low fine material content (<0.074mm). On the other hand, *Baldios* displayed the highest fine material content, having presented more than double the amount of *Cortiçadas de Lavre*.

Figure 3 plots the granulometric curves and the suitability limits recommended in the literature for compressed earth blocks production [3–5]. Overall, *Baldios* is the soil that best fits the range suggested in XP P13-901 [5]. However, *Baldios* seems to be the most promising one. On the other hand, *Cortiçadas de Lavre* is the soil with the fine materials content most deviates from the suitability limits.

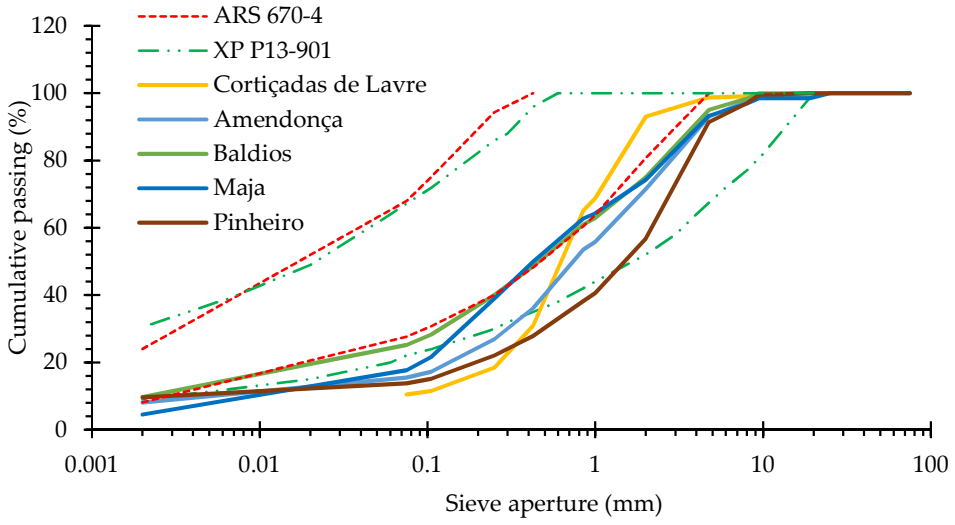

Figure 3 – Diagram of texture for soil for unstabilised and stabilised compressed blocks production [4,5]

Additionally, to assess the clay content (<0.002mm), the jar sedimentation test was performed according to HB195 [6]. Given its considerably low fines content, this test was not performed on *Cortiçadas de Lavre*. A transparent jar with straight sides and flat bottom

was filled up to a quarter of its volume with a sample of soil, which had been previously sieved on a 2mm mesh. Then, the remaining volume of the jar was filled with water and a suitable deflocculant. After the soil was soaked, the jar was vigorously shaken for about 1-2 minutes and left undisturbed for 1 hour. Then, the jar was re-shaken for another minute and placed on a flat surface. After the soil settled in the jar, the fractions were visually identified, and the thickness of the different layers was measured with a ruler (Figure 4).

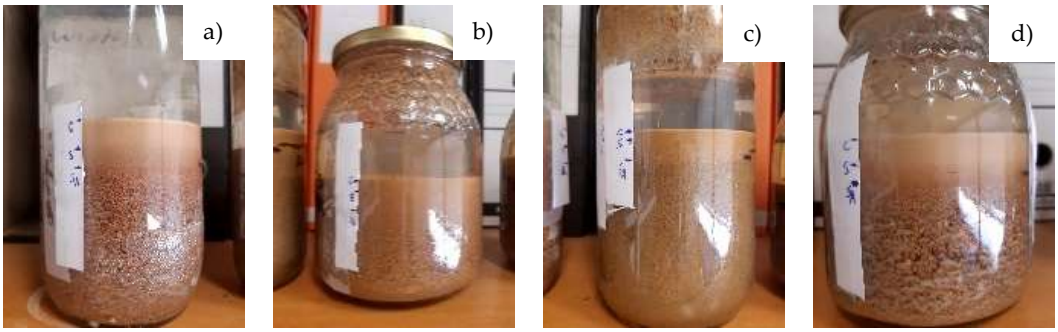

Figure 4 – Jar sedimentation test: a) Amendonça; b) Baldios; c) Maja; d) Pinheiro

Figure 5 presents the soil portions identified in the jar sedimentation tests. It is important to notice that, since the samples were sieved at 2mm, no gravel fraction is identified. Therefore, the results cannot be directly compared with the obtained fractions from the particle size distribution test.

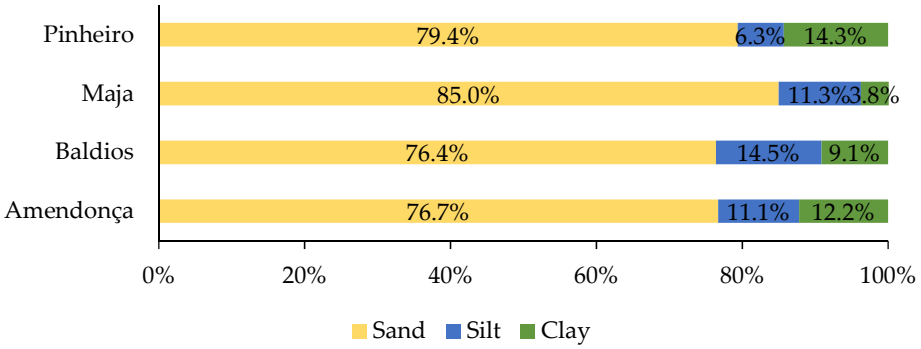

Figure 5 – Jar sedimentation results

The proportion between silt and clay obtained from the jar sedimentation test were applied to the results in the particle size distribution. Therefore, the clay content obtained was 9.7%, 8.1%, 9.6% and 4.5% for the soils *Baldios*, *Amendonça*, *Pinheiro* and *Maja*, respectively. Table 1 presents the resulting granulometric fractions of the soils. Note that this method only provides a rough estimation of the clay content. For the soil selected for this study, a more accurate sedimentation test will be carried out later.

Table 1 – Granulometric fractions of the soils

Fraction	Relative portion (%)				
	Cortiçadas de Lavre	Baldios	Amendonça	Pinheiro	Maja
Clay (<0.002mm)	10.5	9.7	8.1	9.6	4.5
Silt (0.074-0.002mm)		15.5	7.4	4.2	13.2
Sand (4.75-0.074mm)	88.2	69.8	77.5	77.6	75.6
Gravel (>4.75mm)	1.3	5.0	7.0	8.6	6.7

2.2 Atterberg limits

The determination of the *Atterberg* limits was carried out according to portuguese standard NP 143 [7], which involves the identification of the liquidity limit (LL), the plastic limit (PL) and the calculation of the plasticity index (PI). For the determination of the LL, a sample of soil of about 500g was broken apart with a mortar and a rubber pestle and then passed through a #40 sieve. Afterwards, a sample of approximately 100 grams was collected from the material that passed through the sieve. The soil sample was placed in the *Casagrande* shell and mixed with distilled water to obtain a homogeneous paste (Figure 6a), which was then distributed in a layer with a maximum thickness of 1 cm. Subsequently, with the aid of a grooving tool, a 2 mm wide groove was made (Figure 6b). The number of strokes necessary for the sides of the homogeneous paste, separated by the groove, to come together at a length of about 1 cm was recorded. A small sample was collected from the union (Figure 6c), weighed and then dried until constant mass in a ventilated oven at 105-110ºC. The sample was then weighed to determine the water content corresponding to the number of strokes. This procedure was done for four water contents, with the addition of water or dry soil, which resulted on the curves presented in Figure 7. The LL corresponds to the water content obtained for 25 strokes. This test predicts that the number of strokes varies between 10 and 40.

Figure 6 – Liquidity limit determination: a) mixture of soil and water and placement on the *Casagrande* shell; b) 2 mm wide groove; c) collection of the sample

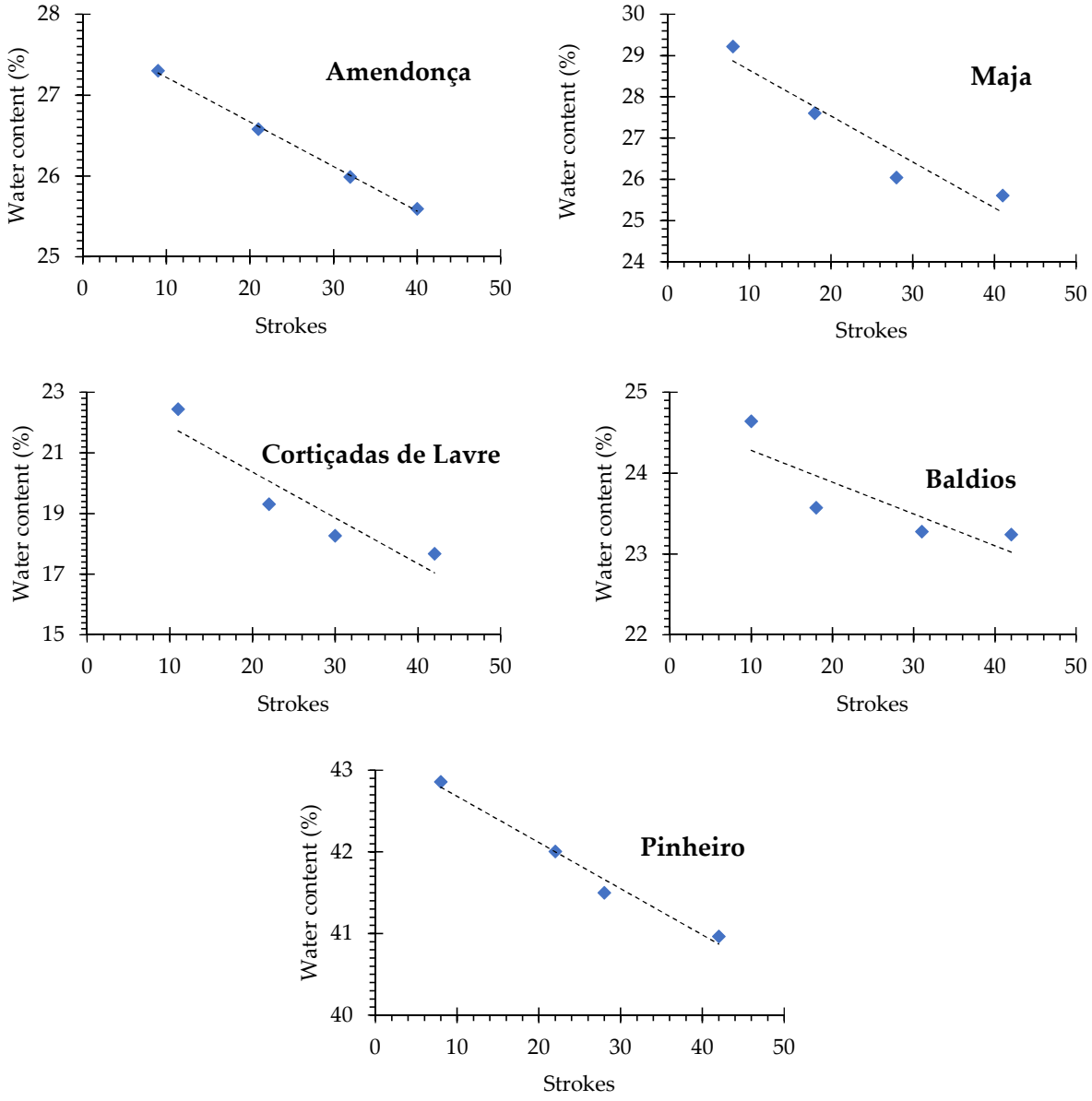

Figure 7 – Relationship between water content and the number of strokes of the soils

The PL was determined from the same sample prepared for the LL. A sample of about 20 g of soil was collected and mixed with increasing amounts of distilled water, until the mixture was sufficiently plastic, allowing four small spheres to be shaped (Figure 8a). Subsequently, the spheres were rolled on a glass plate until cylindrical filaments of 3mm diameter were formed (Figure 8b). The spheres were re-formed, and then rolled again. This procedure was followed until 3mm filaments with small cracks were obtained. The small cracked filaments were placed in containers (Figure 8c), weighed and then placed in a ventilated oven at 105-110ºC, until constant mass. After drying, the sample was weighed again to determine the water content. The PL is the average of the water content

obtained for the four samples. The PI of the soil was obtained by the difference between the values of the LL and the PL.

Figure 8 – Plasticity limit test: a) soil preparation; b) cylindrical filaments with a diameter of 3 mm; c) placement of the samples in capsules

The shrinkage limit (SL) can also be determined using the *Casagrande* method. This limit can be defined as the moisture content at which a soil no longer changes volume upon drying. In this method, the U and A-lines of the plasticity chart (Figure 9) are extended until they converge at a point. Then, a line is extended from that point to the coordinates of the LL and PI. The shrinkage limit is the point where this line crosses the liquid limit axis. Although not an exact procedure, it is reported to be close enough for geotechnical works. The shrinkage index (SI) was obtained by the numerical difference between PL and SL.

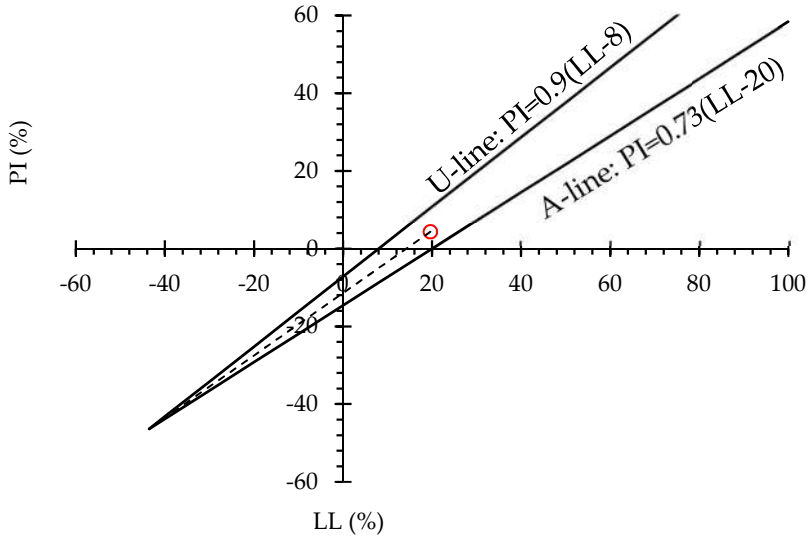

Figure 9 – Shrinkage limit determination
Adapted from Karkush [8]

Table 2 presents the PL, LL, PI, SL and SI of each soil, as well as their USCS classification [9], and expansiveness [10] and activity [11] classifications. Figure 10 shows the Atterberg limits of the studied soils plotted on the plasticity chart, which assisted the USCS classification of the soils. According to the USCS classification, the soils ranged from clayey sand to poorly graded silty clayey sand. The soils were also found to range from slightly expansive to highly expansive (Table 2).

Skempton [11] noted that the PI of a soil increases proportionately with the percentage of clay-size fraction and defined the activity (A) as the ratio of PI to the percentage of the clay-size fraction. A high activity indicates that the soil experiences a significant volume increase when wet and substantial shrinkage when dry. Based on their activity, the soils ranged from inactive to active (Table 2).

Table 2 – Atterberg limits and classifications of the soils

Soil	**LL (%)**	**PL (%)**	**PI (%)**	**SL (%)**	**SI (%)**	**USCS classification** [9]	**Expansiveness classification** [10]	**Activity** [11]	
								A	**classification**
Cortiçadas de Lavre	19.6	15.3	4.3	14.3	1.1	SP-SM-SC (poorly graded silty clayey sand)	Slightly expansive	-	-
Baldios	23.7	18.9	4.7	17.5	1.4	Silty-clayey sand	Moderately expansive	0.49	Inactive
Amendonça	26.4	20.0	6.4	17.9	2.1	Silty-clayey sand	Moderately expansive	0.79	Normal
Pinheiro	41.8	25.4	16.5	19.2	6.1	Clayey sand	Highly expansive	1.72	Active
Maja	27.0	21.8	5.2	19.9	1.9	Silty-clayey sand	Moderately expansive	1.15	Normal

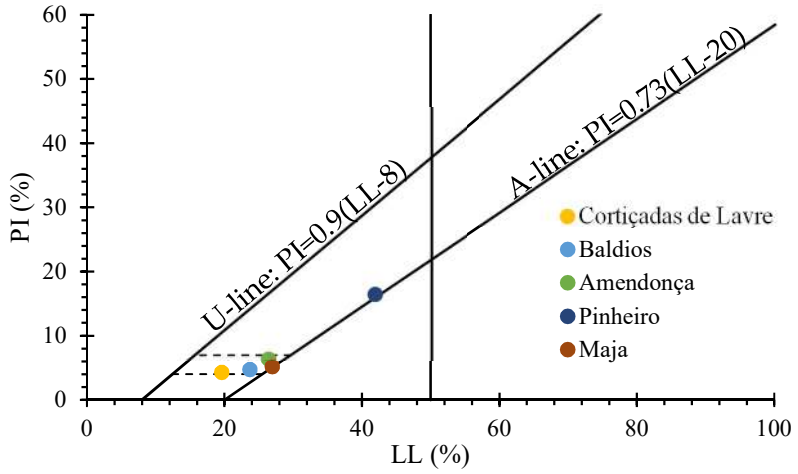

Figure 10 – Liquid limit (LL) vs. plasticity index (PI) of the soils

The Atterberg limits of a soil suitable for compressed earth blocks should preferably fall within the limits of the diagram of plasticity in Figure 11 [5]. This is the case for *Amendonça* and *Maja*, while *Pinheiro* is at the limit of the recommended range. However, considering the ranges proposed by Schroeder [12] (32%≤LL<50% and 17%≤PI<32%), only *Pinheiro* would be considered suitable, while being on the limit of the recommended range for PI.

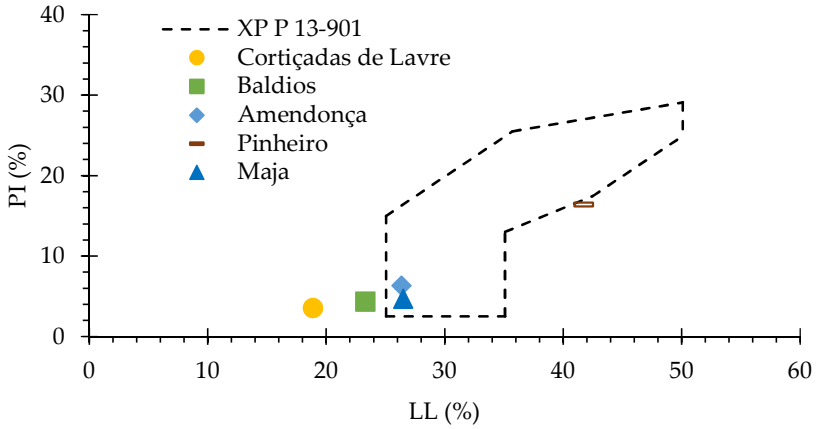

Figure 11 – Soil plasticity chart for unstabilised compressed earth blocks [5]

Table 3 presents the *Atterberg* limits considered adequate for CSEB production proposed in the literature [6,13–15], where some heterogeneity can be found.

To comply with all the suggested considerations, a range of 25-40% for LL and 2-12% for PI is recommended. As a result, the soils *Maja* and *Amendonça* are considered suitable to produce CSEB, while *Baldios* is at the threshold of this new range.

Table 3 – Proposed liquid limit (LL) and plasticity index (PI) by different sources for the production of CEB

Reference	LL (%)	PI (%)
NBR 10833 [13]	≤45	≤18
ARS 1333 [14]	25-46	2-30
Perera [15]	-	≤12
HB 195 [6]	≤40	2-22

2.3 Particle density

The particle density of the soils was determined according to portuguese standard NP 83 [16]. After drying in a ventilated oven at 105-115ºC, a sample of about 100 g of soil was sieved through ASTM sieve #4 and 25g (m_4) were collected. To calibrate the pycnometers, they were filled with distilled water (Figure 12a) up to the reference level and their final mass was recorded (m_3). Then, the dry soil was placed and again filled with distilled water up to about three quarters of its capacity, allowing it to absorb (Figure 12b). After this, the pycnometer was shaken to remove the remaining air and was left to rest for about 24 hours. Distilled water was added back to the reference level and the final mass was recorded (m_5). For a better rigor, the coefficient K that relates the density of water to the temperature at which the assay was performed was determined. The Eq. (1) was applied:

$$\rho = \frac{m_4}{m_3 - (m_5 - m_4)} \quad (1)$$

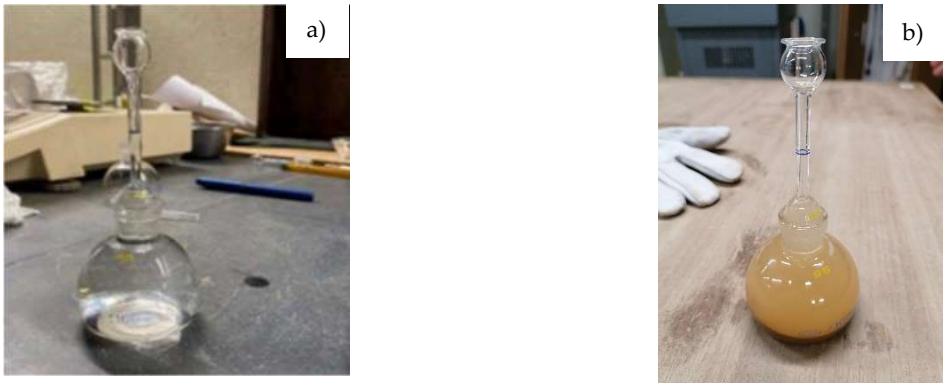

Figure 12 – Determination of the particle density of soils: a) calibration of the pycnometer; b) placement of the soils in the pycnometers

The soils *Cortiçadas de Lavre*, *Baldios*, *Amendonça*, *Pinheiro* and *Maja* presented particle densities of 2530, 2590, 2400, 2510 and 2710 kg/m^3, respectively.

2.4 Optimum moisture content

The optimum water content was determined through the *Proctor* compaction test following ASTM D698 [17]. Firstly, a sample of about 12.5 kg (particle size inferior to 4.75mm) was divided into 2.5 kg portions (Figure 13a). Each portion was then mixed with a pre-established amount of water (Figure 13b). Afterwards, a third of the mixture was introduced in a cylindrical mould (Figure 13c) and compacted with 25 evenly distributed pestle strokes. The process was repeated to make a total of 3 layers. Then, the excess soil was removed (Figure 13d). The mass of the cylindrical mould with the compacted soil (Figure 13e) was recorded, and samples from the interior were taken from both sides and weighed. The samples were dried until a constant mass was reached in a ventilated oven set at 105-110°C. This process was repeated for all five 2.5 kg portions to obtain five points on the compaction curve (Figure 14). For the soils *Cortiçadas de Lavre*, *Maja*, *Pinheiro* and *Baldios*, it was not possible to obtain five 2.5 kg portions due to the lack of soil.

Figure 13 – Compaction test: a) division of the soil into 2.5 kg portions; b) preparation of each portion; c) introduction of the soil in the cylindrical mould; d) excess soil in the mould; e) mould ready for weighing

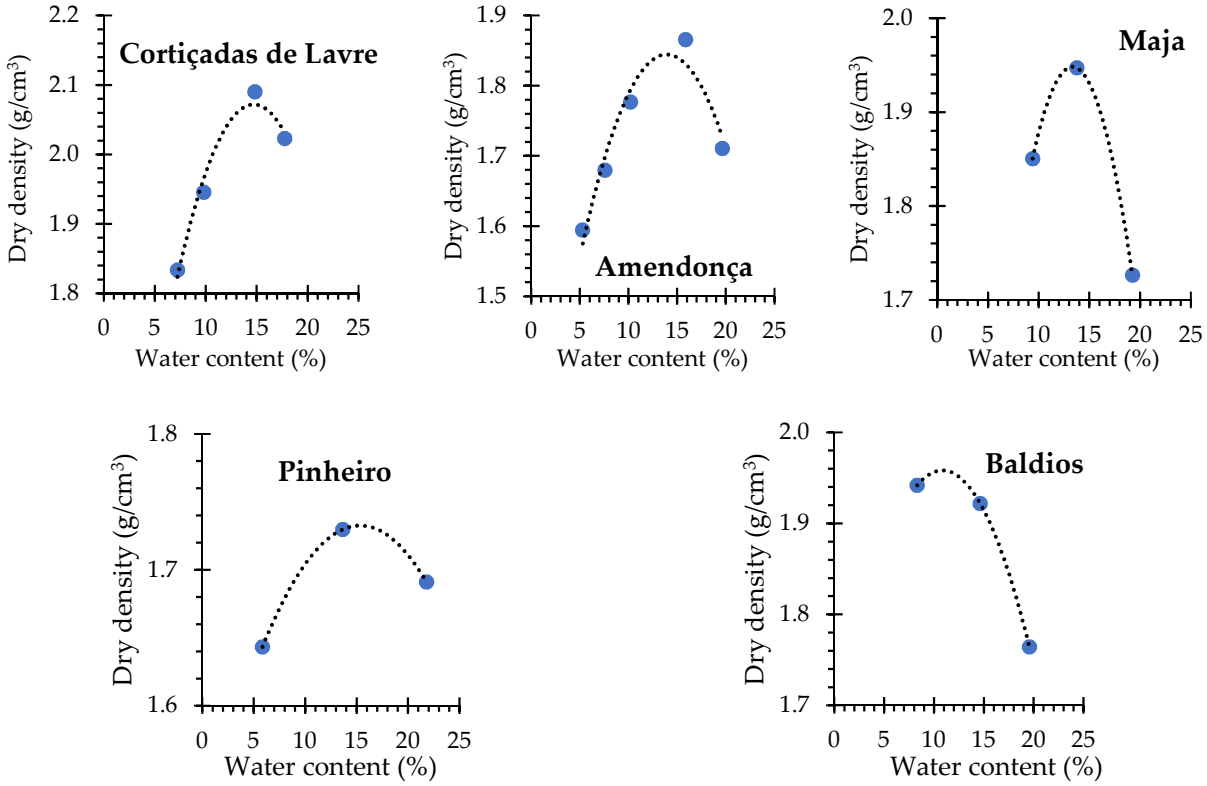

Figure 14 – Compaction curves of the soils

The soils *Cortiçadas de Lavre*, *Baldios*, *Amendonça*, *Pinheiro* and *Maja* presented optimum moisture contents of 14.72%, 10.87%, 13.94%, 15.32% and 13.34%, respectively. These values correspond to maximum dry densities of 2.07, 1.91, 1.84, 1.73 and 1.95 g/cm^3, respectively. Soil *Baldios* had the lowest water requirement and third highest dry density.

2.5 Organic matter

For the determination of the organic matter content (OMC), a sample of about 1 kg was oven-dried at 100°C, until constant mass (m_1) and then mixed with 0.5 L of oxygenated water (H_2O_2) (Figure 15a). After the chemical reaction ended, the sample was oven-dried again until constant mass (m_2) (Figure 15b). The content of organic matter (in percentage) was determined according to Eq. (2).

$$OMC\ (\%) = \frac{|m_2 - m_1|}{m_1} * 100 \quad (2)$$

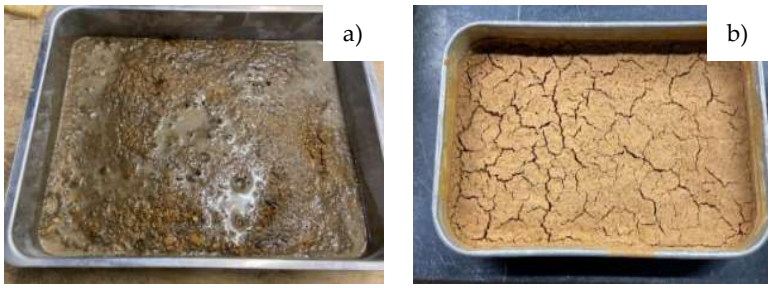

Figure 15 – Determination of the organic matter content: a) mixture of soil with hydrogen peroxide; b) soil after drying

The soils *Cortiçadas de Lavre*, *Baldios*, *Amendonça*, *Pinheiro* and *Maja* presented organic matter contents of 0.30%, 1.48%, 1.02%, 0.34% and 0.43%, respectively.

2.6 X-ray diffraction and thermogravimetric analyses

The X-ray diffraction (XRD) analysis was performed using an *XPERT-PRO* diffractometer (Co Kα source at 1.5406 Å, 40 kV, 35 mA). The XRD patterns were acquired from 5.0437° to 69.9547° 2θ at a step size of 0.033° and a scan step time of 148.0324 s. The identification of the mineral phases was carried out with the *X'Pert HighScore Plus* software.

For each sample, two analyses were carried out, the first one without any kind of pre-treatment and the second one after heating the sample to 450°C. This is done for the correct identification of clay minerals, as the d-spacing at which the peaks of certain types of clays are found undergo a very specific change of position after heating. The identification of clay mineral peaks by means of d-space variations has been carried out using Poppe et al. [18] as a reference.

The different mineral phases identified by XRD analysis are shown in Table 4. The same minerals belonging to the tectosilicate group were common to all the samples: quartz, alibite and microcline. Moreover, soil Maja was the only sample with an amphibole group mineral: hornblende. Finally, the remaining minerals in each sample belong to the phyllosilicate group (also known as clay minerals): kaolinite, montmorillonite, montmorillonite-chlorite, illite, and clinochlore.

In order to correctly identify some types of phyllosilicates, it is not sufficient to identify them with a single XRD analysis, as several clay minerals have the same d-spaces and could be misidentified. For this reason, for each sample, two XRD analyses were carried out, one with the unheated sample and the other one with the sample after having been heated at 450°C (Figures 16-19).

Table 4 – Minerals identified in soils through XRD analysis

Designation	Baldios	Amendonça	Pinheiro	Maja
Minerals	Quartz Albite Kaolinite Microcline Montmorillonite	Quartz Albite Kaolinite Microcline Montmorillonite-chlorite Illite Magnesio-Hornblenda	Quartz Albite Kaolinite Microcline Montmorillonite-chlorite	Quartz Albite Microcline Clinochlore Illite

In soil *Amendonça*, the presence of kaolinite was verified by the existence of a peak at d=7Å in the unheated sample, which was preserved for the sample heated to 450°C. Additionally, the presence of montmorillonite was verified by finding a peak at d=14 Å in the unheated sample, which collapsed at 10 Å in the sample heated to 450°C (Figure 16). In Figure 16, the line representing d=10 Å corresponds to the vertical dashed line with no marked d-value. This is not marked directly on the figure as this data was not obtained directly from the analysis, but it is an interpretation based on observation.

In soil *Maja*, the presence of montmorillonite and kaolinite was verified as in soil *Amendonça*. Moreover, the presence of illite was verified by the existence of a peak at d=10 Å in the unheated sample, which was preserved for the sample heated to 450°C (Figure 17).

In soil *Pinheiro*, the presence of kaolinite and montmorillonite was also identified, as described above (Figure 18).

In soil *Baldios*, the presence of illite was verified as described above (Figure 19). Furthermore, the presence of clinochlorine was rejected. Clinochlore is a phyllosilicate belonging to the chlorite group. The presence of chlorite is consistent with the presence of a peak at d=14 Å in the unheated sample. However, it is discarded when this peak is not preserved for this value of d in the sample heated to 450 °C. Therefore, the interpretation given is that the peak at d= 14 Å in the unheated sample moves to 10 Å in the sample heated to 450 °C. It is therefore interpreted that montmorillonite is present in the sample.

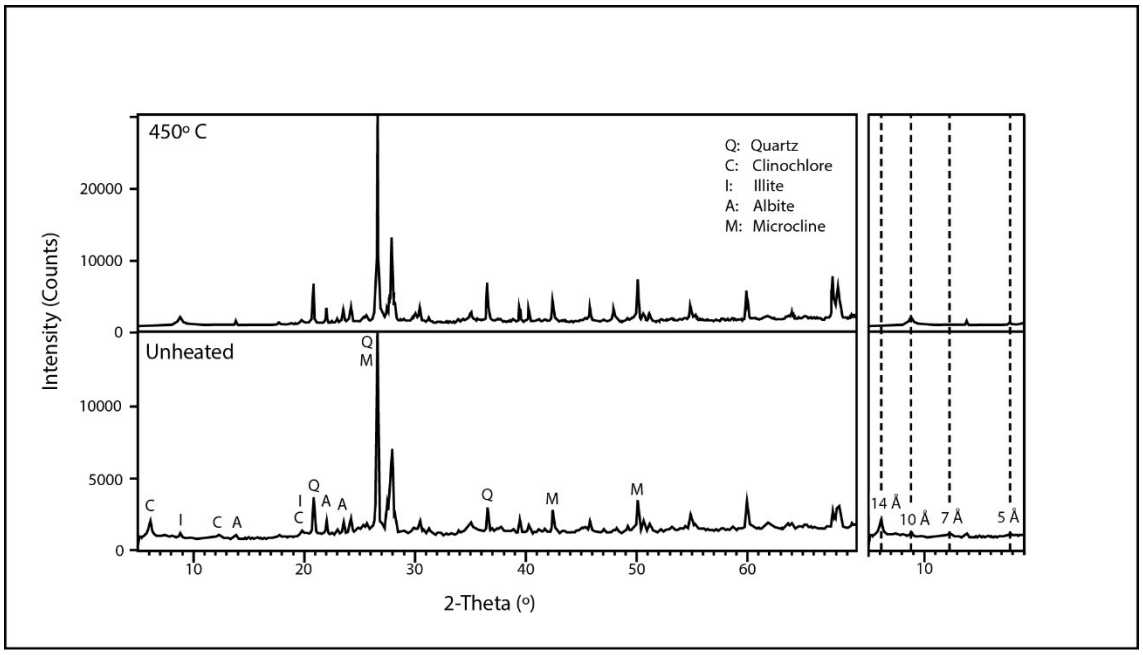

Figure 16 – X-ray diffraction analysis of soil *Amendonça*

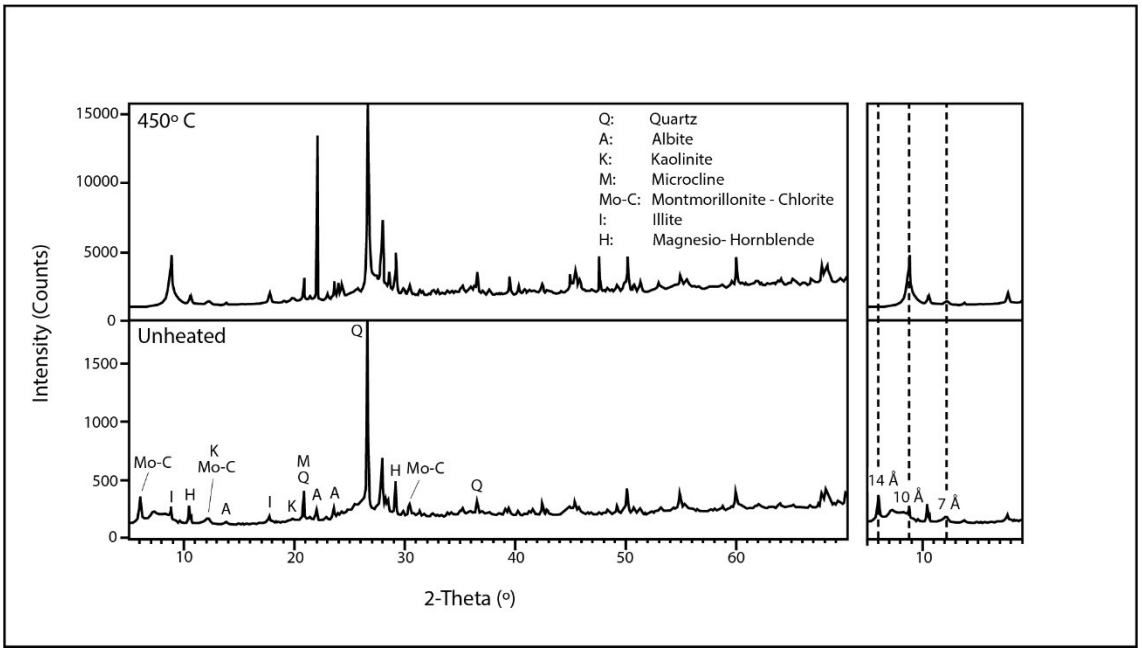

Figure 17 – X-ray diffraction analysis of soil *Maja*

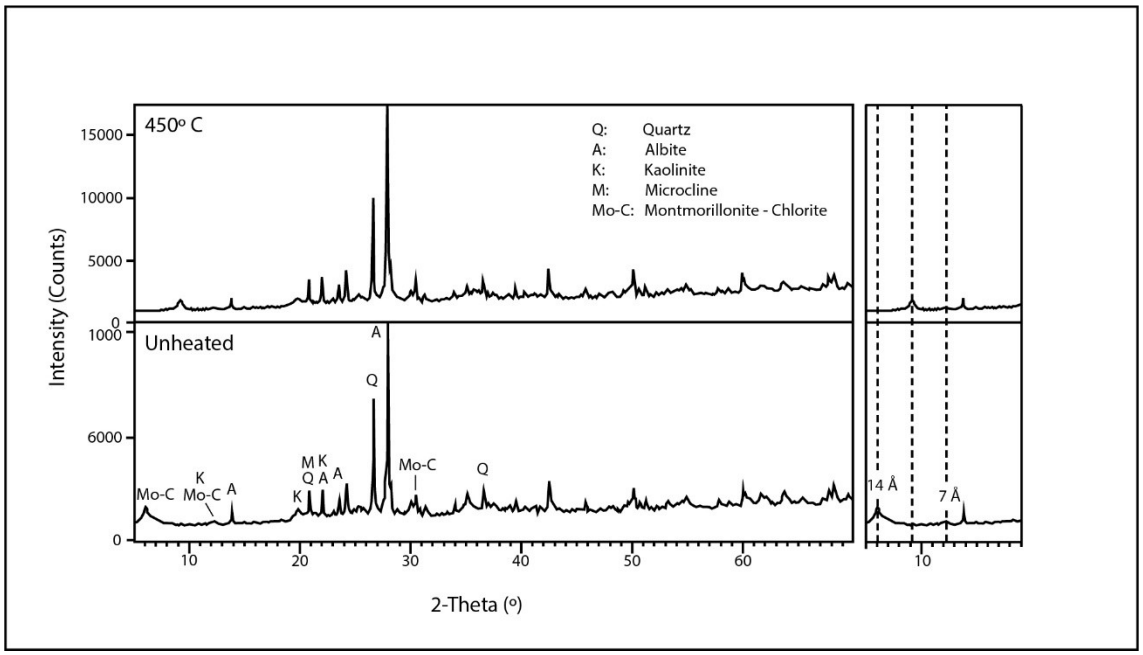

Figure 18 – X-ray diffraction analysis of soil *Pinheiro*

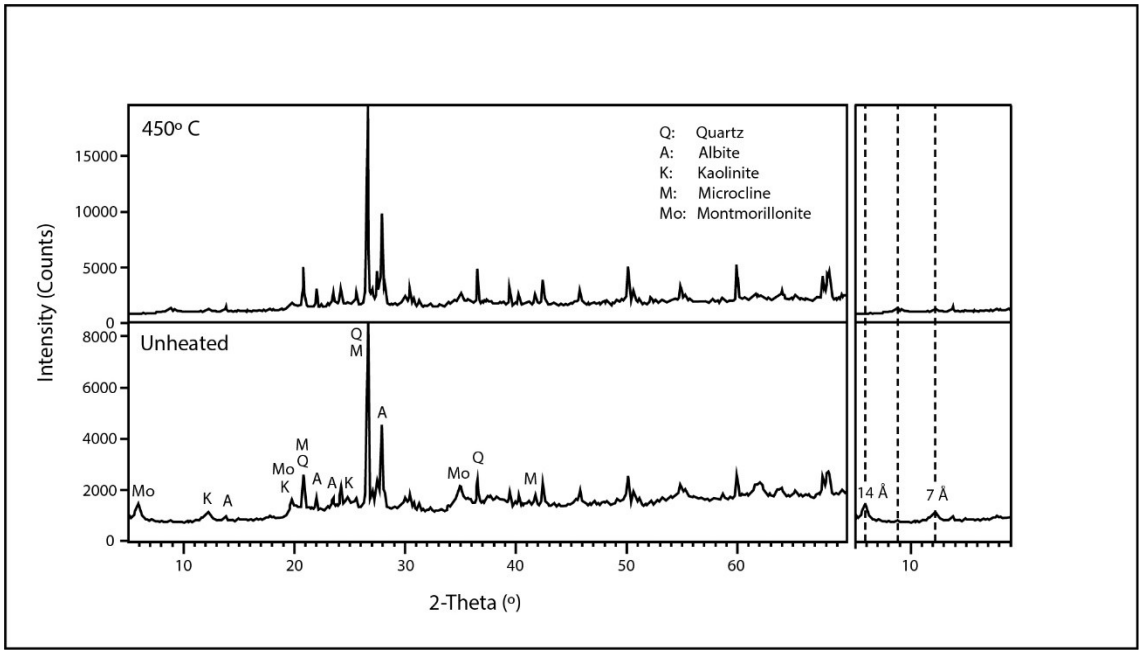

Figure 19 – X-ray diffraction analysis of *Baldios* soil

The thermogravimetric (TG) analysis was performed with a *Hitachi Nexta STA* thermogravimetric analyser. Between 9 and 16 mg of sample were analysed in a platinum

container in flowing nitrogen atmosphere (100mL/min) at a heating rate of 15°C/min from 20 to 950 °C.

The only sample that underwent TG analysis was soil *Baldios* (selected soil). Three different analyses were carried out on different portions of earth from the same sample. It should be noted that the sample did not receive any kind of pre-treatment such as drying before undergoing thermogravimetric analysis.

Both the thermogravimetric curve (TG) and the derivative thermogravimetric curve (dTG) of soil *Baldios* are shown in Figures 20-22. The results (Table 5) show that mass losses occured in two stages. The first state is associated with the dehydration process (when water molecules that are adsorbed on the mineral surface escape under the action of heat) and the second with the dehydroxylation process (when the OH-groups that are part of the mineral structure are released by the action of heat) [19]. Based on the minerals identified in the XRD analysis, this thermal behaviour would be consistent with illite and montmorillonite. Therefore, a more detailed literature review on the thermal behaviour of these two clay minerals was carried out (Table 6).

The first thing that stands out from the thermogravimetric curves is that the loss of water in the first stage occurs abruptly, generating a large peak in the dTG curve which was designated *T1*. This behaviour is associated with the fact that the samples were not dried before carrying out the thermogravimetric analysis, so the water that was supposed to be lost during drying is lost immediately instead of in a more progressive way, generating the *T1* peak in all three analyses. Furthermore, in sample 3, *T1* shows a double peak (Figure 22).

Based on Table 6, the peak temperatures for the dehydration and dehydroxylation phases (*T2* and *T3*) of the three samples would fall within the ranges of both illite and montmorillonite. However, the same is not true for the mass losses at the different stages, given that the mass losses of sample 1 (Figure 20) and sample 3 (Figure 22) were consistent with the thermal behaviour of illite, and those of sample 2 (Figure 21) were closer to the behaviour of montmorillonite.

Taking into account that the analysed samples are soil samples and therefore they are not supposed to be homogeneous, it could be possible that in sample 1 and sample 3, there was an abundance of illite and in sample 2 there was a higher percentage of montmorillonite. XRD analysis also suggest the presence of these two clay minerals. Note

that montmorillonite is an expansive clay mineral, being less adequate for earth construction.

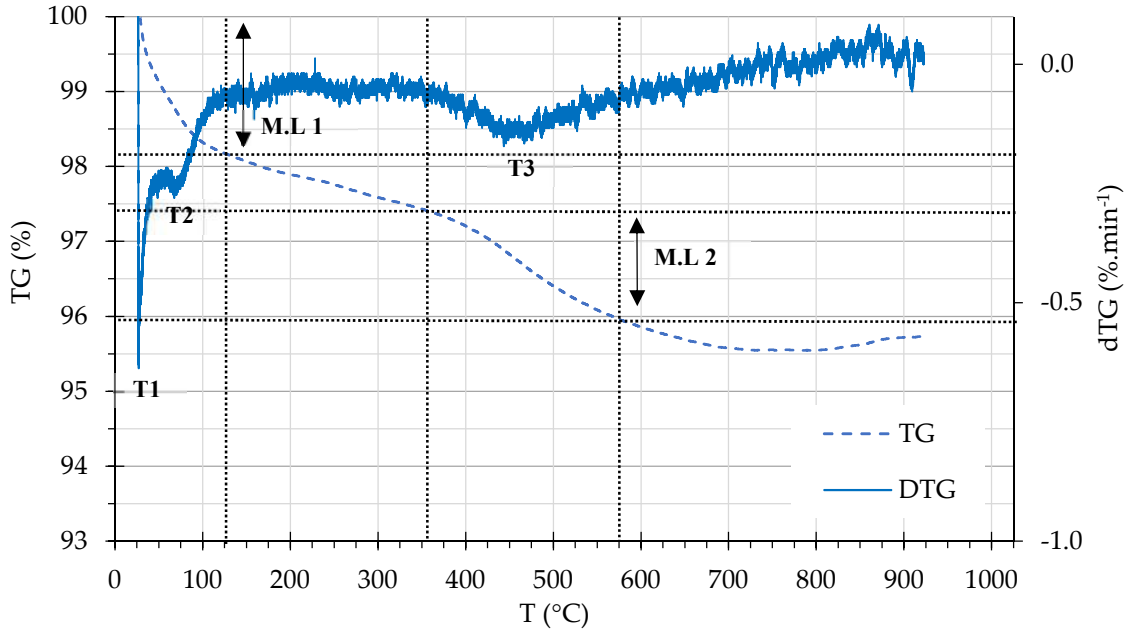

Figure 20 – Thermogravimetric (TG) and differetial TG (dTG) analyses of sample 1 of soil *Baldios*

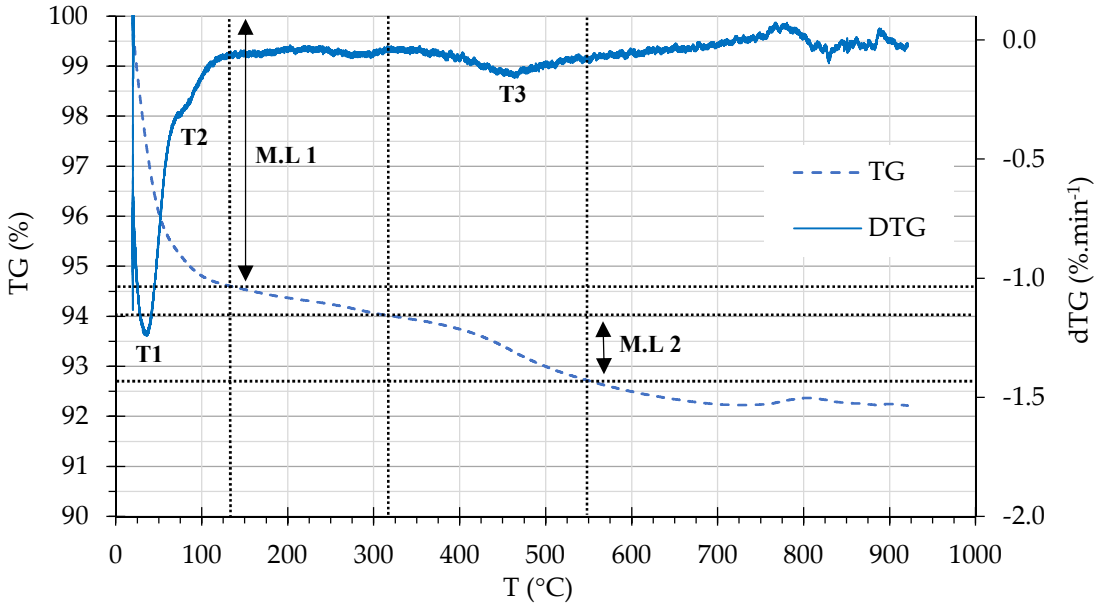

Figure 21 – Thermogravimetric (TG) and differetial TG (dTG) analyses of sample 2 of soil *Baldios*

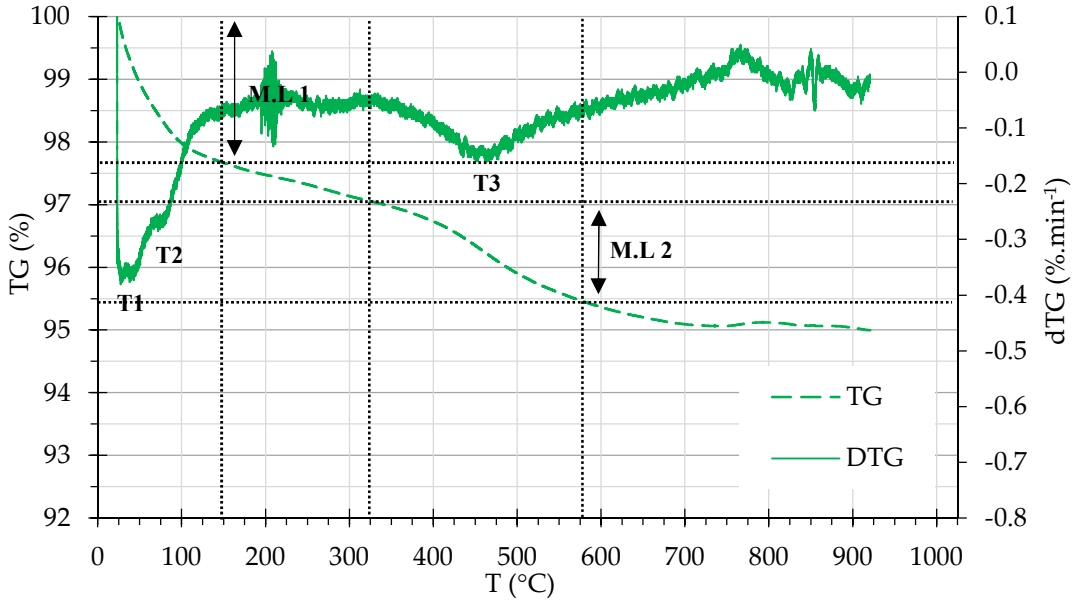

Figure 22 – Thermogravimetric (TG) and differetial TG (dTG) analyses of sample 3 of soil *Baldios*

Table 5 – Results of thermogravimetric analyses of the samples of soil *Baldios*

Designation	**Dehydration**			**Dehydroxylation**	
Baldios	**T1 (°C)**	**T2 (°C)**	**ML (%)**	**T3 (°C)**	**ML (%)**
Sample 1	27	69	1.8	444	1.5
Sample 2	36	73	5.4	461	1.1
Sample 3	29, 45	88	2.3	462	1.43

T – temperature; ML – mass loss

Table 6 – Literature review on temperature and mass loss in the dehydration and dehydroxylation stages in montmorillonite and illite

Mineral	Dehydration		Dehydroxylation		Reference
	T (°C)	ML (%)	T (°C)	ML (%)	
Illite	20-300	-	400-800	-	[20]
	98-114	0.75-1.28	690	2.62-4.66	[21]
	100-200	2.05	About 500	2.25	[19]
Montmorillonite	27-150	11.89	400-600	2.70	[22]
K-Montmorillonite	30-150	4.37	400-600	2.33	
Na-Montmorillonite	30-150	8.36	400-600	2.39	
	100-200	5.94	About 700	2.25	[19]
Ca-Montmorillonite	30-150	10.80	400-600	3.13	[22]
	100-200	7.6; 15.3	About 700	2.6; 3.25	[19]
Mg-Montmorillonite	27-150	11.14	400-600	3.34	[22]

T – temperature; ML – mass loss

3. Conclusions

This report characterised the soils from Montemor-o-Novo to be used in the production of the compressed stabilised earth blocks. Overall, the soils from Montemor-o-Novo did not present optimal characteristics to be used in earth construction, showing expansive clay minerals, low fines content and low values of plasticity index. *Baldios* and *Amendonça* seemed to be the most promising soils. Taking into account the fines content and particle size distribution, *Baldios* showed the best behaviour for the production of CEB.

Acknowledgments

The authors wish to thank the Portuguese Foundation for Science and Technology (FCT) for funding this research through project PTDC/ECI-CON/0704/2021, and under the unit project UIDB/ECI/04625/2020 (CERIS).

References

[1] E 239, Soils. Grain-size analysis by wet sieving, Laboratório de engenharia civil (LNEC), 1970.

[2] E 195, Soils. Dry preparation of specimens for identification tests, Laboratório de engenharia civil (LNEC), 1966.

[3] S. Boubekeur, H. Houben, Compressed earth blocks. Standards, Center for the Development of Industry (CDI) and CRATerre-EAG, 1998.

[4] ARS 670-4, Compressed earth blocks. Part 4: Code of practice for production and construction, African Organization for Standardization (ARSO), 2014.

[5] XP P 13-901, Compressed earth blocks for walls and partitions. Definitions. Specifications. Tset methods. Delivery acceptance conditions, Association Française de Normalisation (AFNOR), 2001.

[6] HB 195, The australian earth building handbook, Standards Australia, 2012.

[7] NP 143, Solos. Determinação dos limites de consistência, Instituto Português da Qualidade (IPQ), 1969.

[8] M. Karkush, Lectures of Soil Mechanics, 2018.

[9] ASTM D2487, Standard practice for classification of soils for engineering purposes (unified soil classification system), American Society for Testing & Materials (ASTM), 2017.

[10] B. Hargreaves, The examination of a possible relationship between the liquid limit (LL%) and soil shrink index (Ips), in: Common Gr. Proceedings. 10th Aust. New Zeal. Conf. Geomech. Brisbane, 2007: pp. 224–229.

[11] A. Skempton, The Colloidal Activity of Clays, in: Proc. Third Int. Conf. Soil Mech. Found. Eng., 1953: pp. 57–61.

[12] H. Schroeder, Modern earth building codes, standards and normative development, in: Mod. Earth Build. Mater. Eng. Constr. Appl., Woodhead Publishing Limited, 2012: pp. 72–109.

[13] NBR 10833, Manufacture of brick and block of soil-cement with use of a manual or hydraulic brickmaking machine. Procedure, Associação brasileira de normas técnicas (ABNT), 1989.

[14] ARS 1333, Compressed stabilized earth blocks. Requirements, production and construction, African Organization for Standardization (ARSO), 2018.

[15] A. Perera, Innovations, applications and standards of compressed stabilised earth blocks (CSEB), in: Glob. Innov. Constr. Conf. Loughborough, United Kingdom, 2009: pp. 154–162.

[16] NP 83, Soils. Determination of particle density, Instituto Português da Qualidade (IPQ), 1965.

[17] ASTM D698, Standard Test Methods for Laboratory Compaction Characteristics of Soil Using Standard Effort (12,400 ft-lbf/ft3 (600 kN-m/m3)), American Society for Testing & Materials (ASTM), 2021.

[18] L. Poppe, V. Paskevich, J. Hathaway, D. Blackwood, Laboratory Manual for X-Ray Powder Diffraction, 2001.

[19] M. Földvári, Handbook of thermogravimetric system of minerals and its use in geological practice, Geological Institute of Hungary, 2011.

[20] T. Húlan, A. Trník, I. Štubňa, P. Bačík, T. Kaljuvee, L. Vozár, Development of young's modulus of illitic clay during heating up to 1100°C, Mater. Sci. 21 (2015) 429–434. https://doi.org/10.5755/j01.ms.21.3.7152.

[21] B. Erdoğan Alver, G. Dikmen, Ö. Alver, Investigation if the influence of heat treatment on the structural properties of illite-rich clay mineral using FT-IR, 29Si MAS NMR, TG and DTA methods, Anadolu Univ. J. Sci. Technol. A - Appl. Sci. Eng. 17 (2016) 823–823. https://doi.org/10.18038/aubtda.279851.

[22] A. Elkhalifah, S. Maitra, M. Bustam, T. Murugesan, Thermogravimetric analysis of different molar mass ammonium cations intercalated different cationic forms of montmorillonite, J. Therm. Anal. Calorim. 110 (2012) 765–771. https://doi.org/10.1007/s10973-011-1977-8.

Report Eco+RCEB/R1

Characterisation of materials: Soils from Montemor-o-Novo

Lisbon, 31 of March 2023

Authors

Sofia Real

Researcher
(IST)

Ricardo Cruz

PhD student
(IST)

Andrea Balboa

PhD student
(IST)

Manuel F.C. Pereira

Assistant Professor
(IST)

José Alexandre Bogas

Assistant Professor
(IST)